



Institut für Experimentalphysik an der KFU Graz

Übungstitel: Light tweezers

Supervisor: Peter Banzer, Univ.-Prof. Dr.rer.nat.

Gruppennummer:	Vorbereitung	Durchführung	Protokoll	Σ

Name: Maximilian PHILIPP **Mat. Nr:** 11839611

Name: Matthias STARK **Mat. Nr:** 12004907

Contents

1	Tasks	3
2	Basic concepts	3
2.1	Brownian Motion and Its Relation to Diffusion	3
2.2	Fick's Law of Diffusion	3
2.3	Einstein Relation (Einstein-Smoluchowski Equation)	4
2.3.1	Derivation of the Einstein Relation from Fick's Law	4
2.4	Optical Trapping	5
2.4.1	Rayleigh Regime	6
2.5	Mie Regime	6
2.6	Momentum Transfer	7
2.6.1	Angular Momentum Transfer	8
3	Experimental Setup	10
4	Materials	12
5	Measurement and Analysis	12
5.1	Microscope	13
5.2	Lasergun	19
5.3	Trapping with laser	19
5.4	Holding force	22
5.5	Characterization of unknown sample	24
5.6	Trapping of living organisms	24
5.7	Transfer of angular momentum	25
6	Discussion	25
6.1	Microscope	25
6.2	Lasergun	26
6.3	Trapping with laser	26
6.4	Holding force	26
6.5	Characterization of unknown sample	26
6.6	Trapping of living organisms	27
6.7	Transfer of angular momentum	27
7	Conclusion	28

1 Tasks

During the experiment the following steps need to be performed:

- Build a microscope and observe forces on microscopic particles without a laser
- Use the laser as a "gun" to hit some microscopic particles
- Trap particles with the laser beam
- Trap "living" organisms
- Transfer angular momentum to a particle

2 Basic concepts

2.1 Brownian Motion and Its Relation to Diffusion

Brownian Motion is the random, erratic movement of particles suspended in a fluid, discovered by Robert Brown in 1827. This motion results from collisions with the molecules of the surrounding medium, which are in constant thermal motion.

Diffusion Constant (D) quantifies how fast particles diffuse in a medium. It is influenced by the temperature of the medium, the viscosity, and the size of the diffusing particles.

Average Squared Displacement (ASD) measures how far particles move from their original position, on average, over time. Mathematically, it is expressed as:

$$\langle (\Delta x)^2 \rangle = 2dDt \quad (1)$$

where $\langle (\Delta x)^2 \rangle$ is the mean squared displacement, d is the dimensionality of motion, D is the diffusion constant, and t is time.

2.2 Fick's Law of Diffusion

Fick's Law describes the flux of particles under a concentration gradient:

2.2.0.1 Fick's First Law: Indicates that the particle flux J is proportional to the negative of the concentration gradient ∇c :

$$J = -D\nabla c \quad (2)$$

2.2.0.2 Fick's Second Law: Describes the time dependence of concentration due to diffusion:

$$\frac{\partial c}{\partial t} = D \nabla^2 c \quad (3)$$

This law shows how the concentration changes in response to the diffusion spread, balancing out concentration differences over time.[7]

2.3 Einstein Relation (Einstein-Smoluchowski Equation)

The Einstein relation connects diffusion with the microscopic random motion observed in Brownian motion. Einstein derived a formula linking the diffusion constant D with temperature T , the Boltzmann constant k_B , and the mobility μ of the particles:

$$D = \mu k_B T \quad (4)$$

2.3.1 Derivation of the Einstein Relation from Fick's Law

2.3.1.1 Equilibrium State: Starting with Fick's First Law under the assumption of thermal equilibrium and a potential energy $U(x) = -Fx$ due to a small applied force F :

$$\begin{aligned} c(x) &= c_0 e^{\frac{F_x}{k_B T}} \\ \nabla c &= \frac{F}{k_B T} c(x) \\ \Rightarrow J &= -D \frac{F}{k_B T} c(x) \end{aligned}$$

2.3.1.2 Mobility: By definition, mobility μ is the velocity per unit force. Express the flux J also as $J = \mu F c(x)$.

2.3.1.3 Equating Fluxes: Equating the two expressions for J :

$$\begin{aligned}\mu F c(x) &= -D \frac{F}{k_B T} c(x) \\ \mu &= -\frac{D}{k_B T} \\ D &= \mu k_B T \quad \# \text{with absorption of the sign into the definition of } \mu\end{aligned}$$

for spherical particles in a liquid with low Reynolds number one substitute the mobility using the Stokes law for the frictional force:

$$\begin{aligned}F_{\text{Stokes}} &= 6\pi\eta Rv \\ \mu &= \frac{F}{v} = 6\pi\eta R\end{aligned}$$

and arrive at the Stokes–Einstein–Sutherland equation.[5]

$$D = \frac{k_B T}{6\pi\eta R} \quad (5)$$

Lastly one can equate the Brownian motion and the diffusion constant to get the:

$$\langle (\Delta x)^2 \rangle = 2d \frac{k_B T}{6\pi\eta R} t \quad (6)$$

using the differential form: (7)

$$d \langle (\Delta x)^2 \rangle = \frac{dk_B T}{3\pi\eta R} dt \quad (8)$$

$$\Rightarrow \frac{\partial \langle (\Delta x)^2 \rangle}{\partial t} = \frac{dk_B T}{3\pi\eta R} \quad (9)$$

2.4 Optical Trapping

Overarching principle: due to the Gaussian form of the laser beam there exists a stable location along the beam near the waist of the beam where particles are attracted to. This fixes the position of particles in the first axis. How the other two degrees of freedom are fixed is dependent on the particle size and explained below:

2.4.1 Rayleigh Regime

In the Rayleigh regime, the particle size is much smaller than the wavelength of the trapping light (usually less than about one-tenth of the wavelength). Here, the particle can be modeled as an electric dipole induced by the electric field of the light.

2.4.1.1 Gaussian Beam: A Gaussian beam, typically used in optical trapping, has a highly focused, bell-shaped intensity profile. The electric field of such a beam varies spatially, being strongest at the center and decreasing towards the edges.

2.4.1.2 Dipole Interaction and Gradient Force: The particle in a Gaussian beam experiences an induced dipole moment due to the electric field. This dipole moment ($\vec{p} = \alpha \vec{E}$) is proportional to the electric field \vec{E} , where α is the particle's polarizability.

The key force at work here is the gradient force, which arises due to variations in the light's electric field intensity. The force \vec{F} on the dipole is given by:

$$\vec{F}(\vec{p} \cdot \nabla) \vec{E} \quad (10)$$

This equation shows that the dipole (the particle) is attracted towards regions of higher electric field intensity. In the Gaussian beam, this means the particle is pulled towards the beam's center, effectively trapping it at the focus where the intensity is maximal. This fixes the other two degrees of freedom of the particle.[4]

2.5 Mie Regime

Mie theory is valid for all relative particle sizes to the wavelength. This theory would require considering the full solution to Maxwell's equations for the interaction between light and the sphere, leading to more complex behaviors than in the Rayleigh regime.

2.5.0.1 Geometrical Optics in Mie Regime: When the particle size is comparable to or larger than the wavelength of light then the geometric optics approximation can be used here, where the trapping light can be considered as rays that get refracted and reflected as they interact with the sphere. Each light ray imparts momentum to the particle according to the change in the ray's momentum (light pressure).

2.5.0.2 Gradient Force: As in the Rayleigh regime, the gradient force still plays a crucial role but its calculation becomes more complex due to the detailed interaction of light rays with the particle. The distribution of light around the sphere creates regions of varying intensity and gradient, and the sphere tends to move towards the region of highest intensity. The geometrical momentum transfer and gradient force is visualized below.[4]

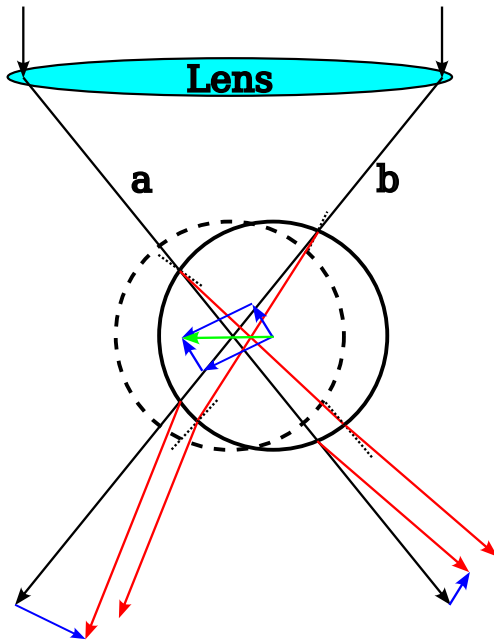


Figure 2.1: In black the original undisturbed rays are visible in red the rays refracted due to the solid sphere. The dashed circle depicts the resting position of the sphere and is the point where momentum transfer due to refraction is symmetric and horizontal components cancel. In blue one can see the momentum difference due to the refraction for the left and the right beam. Once the negative momentum are added one can see the trapping force acting on the sphere (in green).

2.6 Momentum Transfer

Photons are quantum particles of light and carry energy and momentum despite having no mass. The momentum p of a photon is related to its wavelength λ and energy E [6]. The momentum of a photon is given by the equation:

$$p = \frac{E}{c} \quad (11)$$

2.6.0.1 Light Beam as a Stream of Photons A beam of light can be described as a stream of photons, each carrying energy and momentum. When considering a beam of light, you can sum the momenta of individual photons to understand the total momentum of the beam.

When light (photons) bends due to refraction, there's a change in the direction of the photons' momentum. Since momentum is a vector quantity, any change in direction implies a change in momentum.

If we consider the force \vec{F} as the rate of change of momentum $\frac{\partial \vec{p}}{\partial t}$ then a bending photon experiences a force due to its changing momentum. According to Newton's third law, if the photon experiences a force the opposite force is experienced by the object . Since a force is defined as the time rate of change of momentum $\vec{F} = \frac{\partial \vec{p}}{\partial t}$, and a beam of light is a stream of photons each changing momentum upon interaction with an object, the beam itself exerts a force. This is observable in phenomena such as radiation pressure, where light exerts pressure on surfaces due to momentum transfer from photons.[4]

2.6.1 Angular Momentum Transfer

To receive angular momentum and start spinning from polarized light, a microscopic particle typically needs to exhibit certain properties such as birefringence, non-spherical shape, and the ability to interact with the specific polarization state of the incident light.

2.6.1.1 Birefringence: Birefringent particles can interact with polarized light to convert the angular momentum of the photons into mechanical rotation. When a birefringent particle is placed in an optical trap and illuminated with circularly polarized light, the transfer of spin angular momentum can induce rotation. Transparent birefringent particles like calcite can spin with high rotation frequencies without overheating due to their transparency.[8]

2.6.1.2 Non-Spherical Shape: Non-spherical particles, such as irregularly shaped birefringent particles, show different rotational behaviors under polarized light. These particles can exhibit periodic acceleration and deceleration due to varying spin angular momentum transfer from the light.[12]

2.6.1.3 Interaction with Polarization State: The state of polarization of the incident light (linear, circular, or elliptical) affects how the angular momentum is imparted to the particle. For instance, particles exposed to a circularly polarized light beam can experience both spinning and orbital motion around the beam axis, as demonstrated in experiments with Gaussian beams. [1]

2.6.1.4 Absorption and Optical Properties: The optical properties of the particles, such as absorption and refractive index, also play a significant role. For instance, gold nanoparticles can achieve very high rotation frequencies when illuminated with circularly polarized light due to their favorable optical properties and the low local viscosity caused by particle surface heating. [10]

3 Experimental Setup

The total setup of the experiment is visible in Figure 3.1. In general it depends on several cage modules, that were used for the single steps.

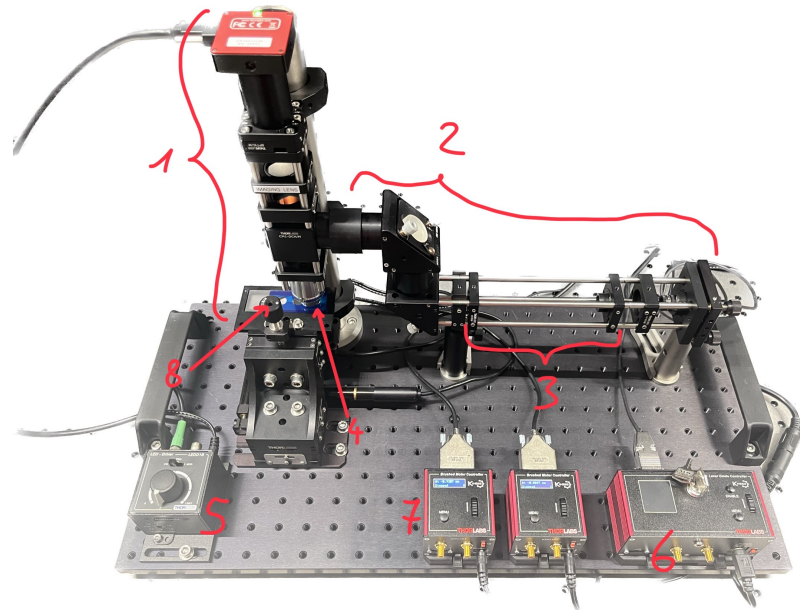


Figure 3.1: Total experimental setup

- 1 ...Microscope module
- 2 ...Laser module
- 3 ...Telescope module
- 4 ...Sample stage
- 5 ...Power supply for light
- 6 ...Power supply for laser
- 7 ...Controller for movement of the sample in x/y-direction
- 8 ...Screw for movement of the sample in z-direction

The single optical components, as well as the beampath are visible in Figure 3.2.

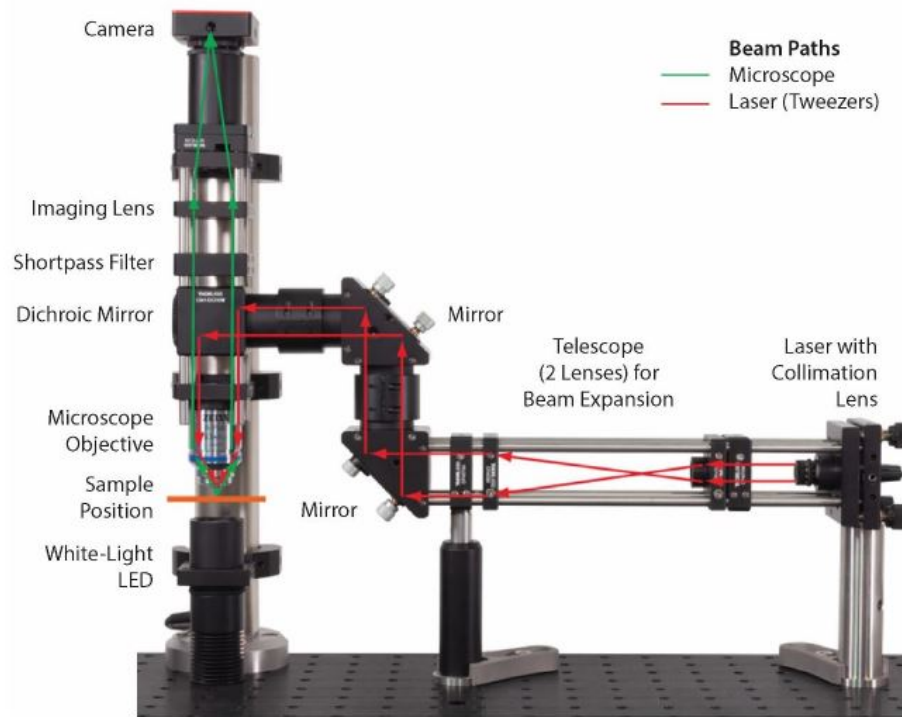


Figure 3.2: Optical setup with drawn beam-path [3]

4 Materials

For the setup the following parts in Table 4.1 are used.

Table 4.1: Used parts for the experiment

Device	Producer	type	Sidemark
Camera	ThorLabs	CS165CU/M	
Imaging Lens	ThorLabs		
Shortpass Filter	ThorLabs		
Dichroic Mirror	ThorLabs		
Microscope Objective	Zeiss	421080-9900	63x
Sample Holder			
White-Light LED	ThorLabs	LEDD18	
Mirror	ThorLabs		2x
2 Lenses	ThorLabs		as Telescope
Collimator Lens	ThorLabs		
Laser	ThorLabs	Kinesis	
Brushed Motor Controller	ThorLabs		for navigation of sample
Stage	ThorLabs		
Breadboard	ThorLabs		

5 Measurement and Analysis

In order to see how the uncertainty of the measurements propagates into the results, the extended Gauss method was used. For the analysis python was used in combinations with the packages `scikit-learn`, `numpy`, `opencv`, `scipy`, `matplotlib` and `uncertainties`.

In order to ensure the highest possible accuracy, the values are not rounded until they are displayed in tables.

Regarding the images it is very important to save them in the correct format, so that they can be displayed later.

5.1 Microscope

For this part only the microscope module form Figure 3.1 is needed.

As a sample the Silicas are used. The object holder has a thin placeholder on it, so that the tiny particles in the liquid are allowed to move, as visible in Figure 5.1

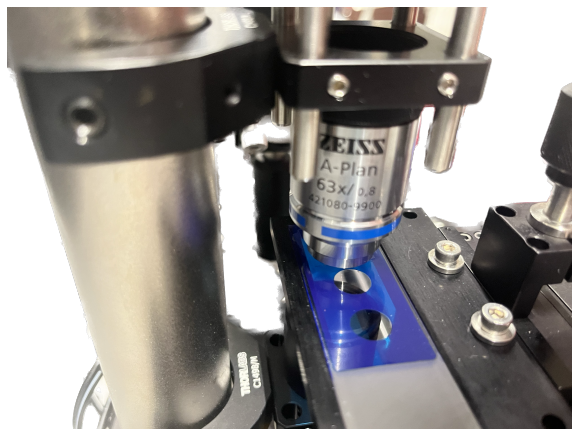


Figure 5.1: Object holder with placeholder

The object holder is placed on the specimen stage and the camera is connected with the computer. The analyse of the sample is done with the "ThorCam" software. It is important to make sure that there is enough space between the sample and the detector, to avoid a crash.

Now the white light LED under the sample is switched on in order to create an image on the software. It is important to keep in mind, that there is a filter between the sample and the camera to protect it later from the direct incident of the laser. That's why the image appears in a greenish shine. Now the sample is slowly moved upwards in z-direction to create a sharp image.

If the focus is set right, one can observe the Brownian motion of the small particles. Some of them stand still, because they are attached either to the objective holder or to the cover glass. With the electric controller one can now navigate over the sample, by selecting an appropriate speed in the menu.

To measure the Brownian motion one needs a position on the sample where one finds at least 3 moving particles at approximately the same size. Then one records the screen for at least 2 min to make an analyse of the movement of the particles. One of these spots is visible in Figure 5.2 and Figure 5.3, as an example. The same procedure is again carried out for another spot.

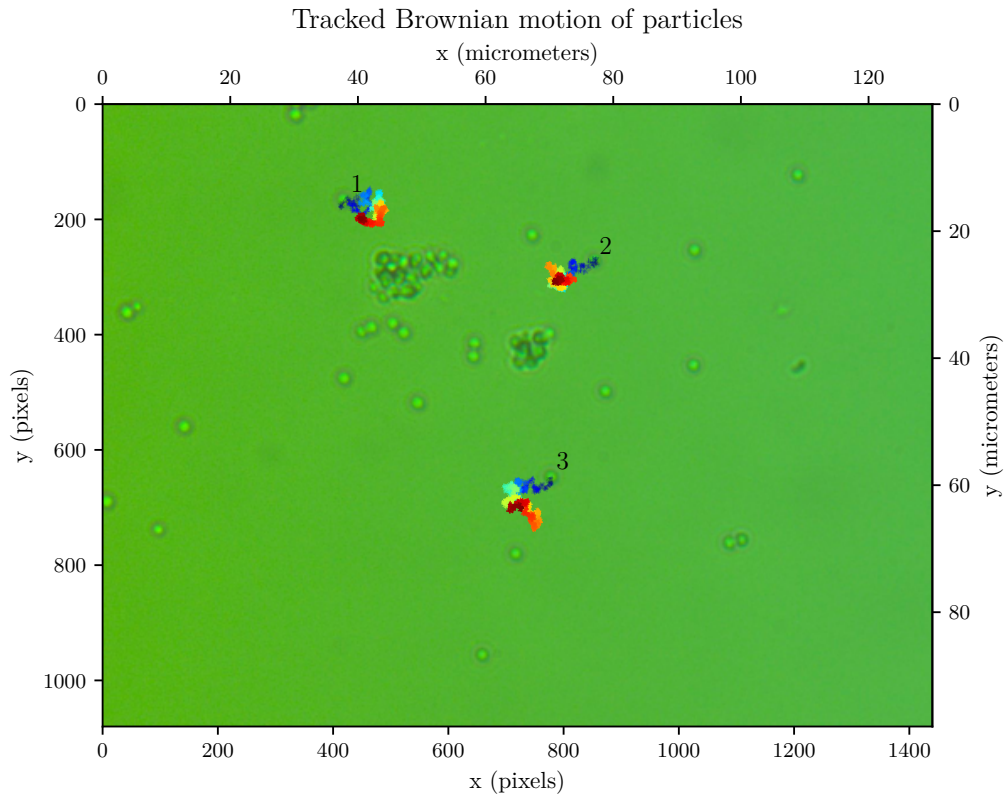


Figure 5.2: This figure contains the initial conditions of the tracked region displayed in the background and has the trajectories of the particles overlaid from cold to hot indicating the time evolution of the particles. Furthermore, the particles are labeled and plotted on an x, y coordinate grid. This is the first capture of particles.

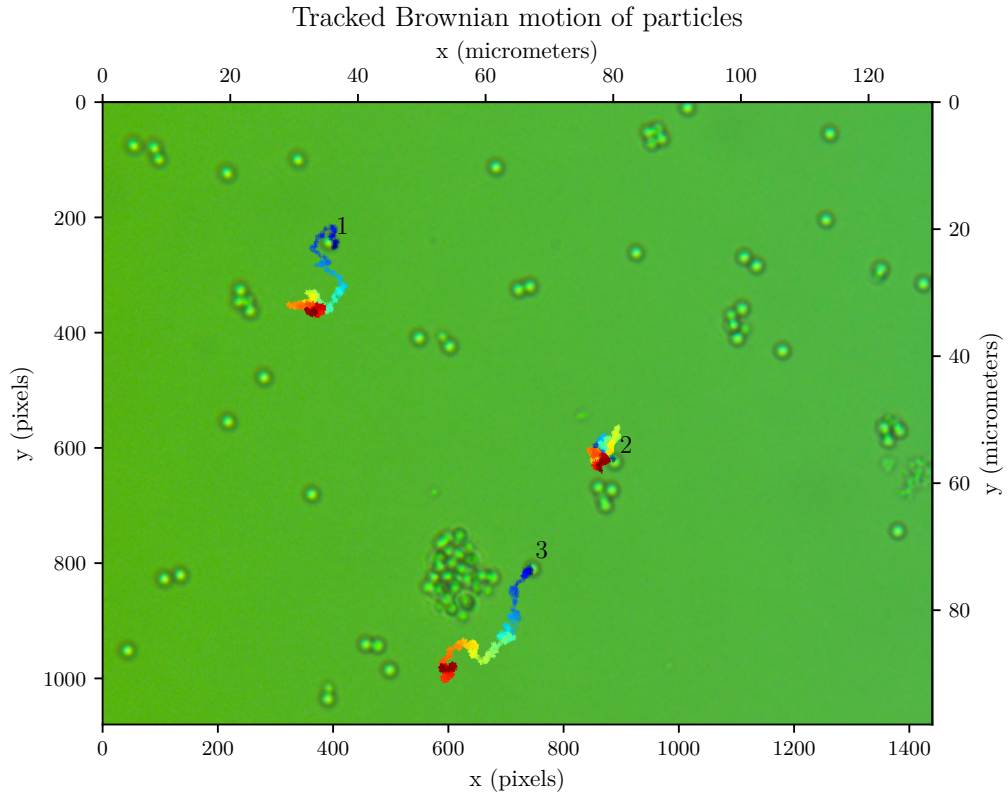


Figure 5.3: This figure contains the initial conditions of the tracked region displayed in the background and has the trajectories of the particles overlaid from cold to hot indicating the time evolution of the particles. Furthermore, the particles are labeled and plotted on an x, y coordinate grid. This is the second capture of particles.

Using the trajectories of the particles one can now calculate the effective viscosity η_{eff} of the liquid using the mean squared displacement. The effective viscosity is calculated using the rate of change of the mean squared displacements s . Solving the Equation 9 for the effective viscosity η_{eff} one gets:

$$\eta_{\text{eff}} = \frac{2k_B T}{3\pi s R} \quad (12)$$

But firstly one needs to calculate the mean squared displacements s for each of the particle trajectories.

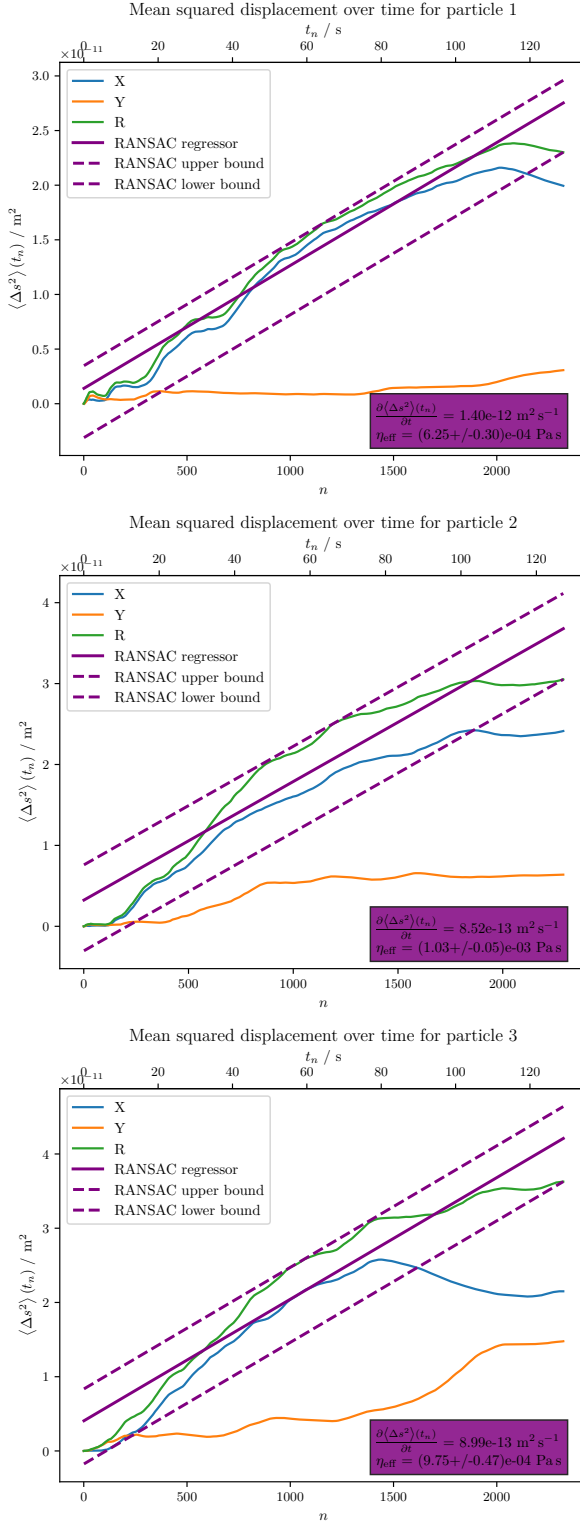


Figure 5.4: This figure one can see the time averaged mean squared displacements ($\langle \Delta s^2 \rangle(t_n)$) (averaged up to every time step t_n) in X and Y direction and the radial direction R. The labels correspond to particles in Figure 5.2.

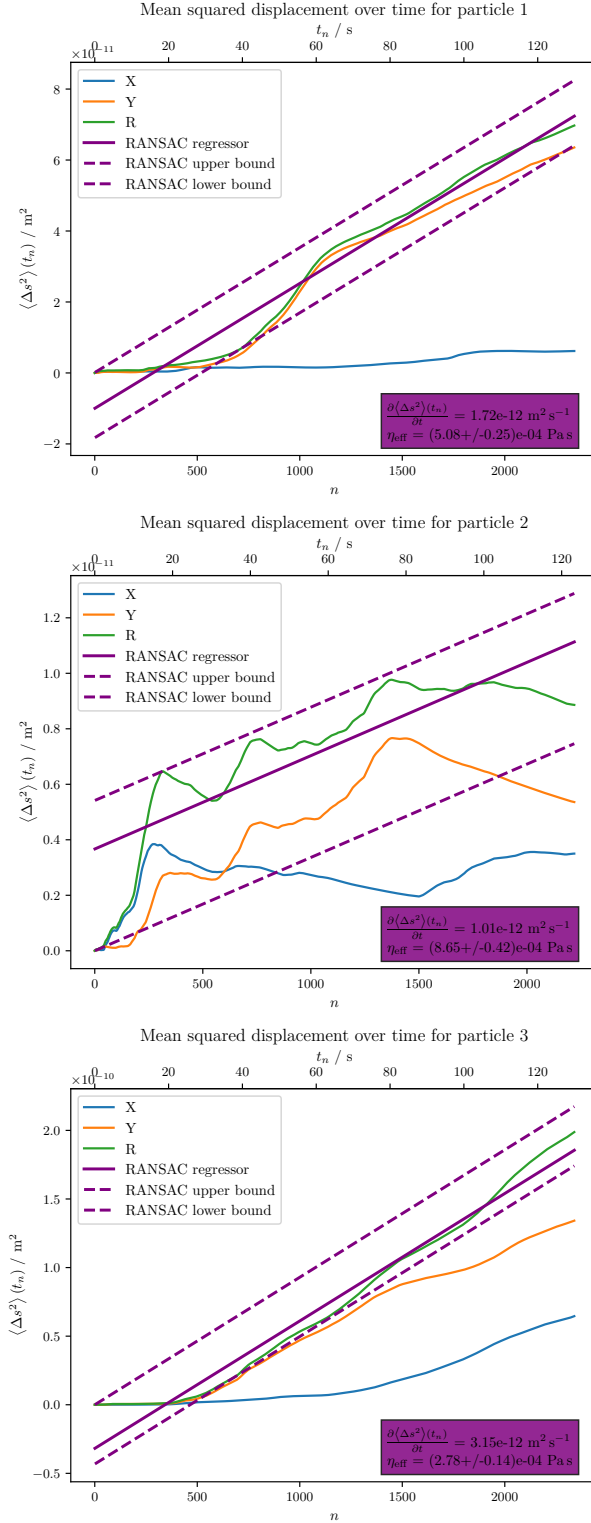


Figure 5.5: This figure one can see the time averaged mean squared displacements ($\langle \Delta s^2 \rangle(t_n)$) (averaged up to every time step t_n) in X and Y direction and the radial direction R. The labels correspond to particles in Figure 5.3.

Using the slope of the fitted lines s , the radius of the spherical particles $R = 2,06 \mu\text{m}$ and the medium temperature of $T = (308,15 \pm 15,00) \text{ K} = (35 \pm 15)^\circ\text{C}$ we can calculate the effective viscosity η_{eff} . Here the temperature was assumed to be the 20°C above the room temperature. Since the irradiance of lamp was heating up the liquid. This is the only uncertainty considered in the calculation of η_{eff} . Since the RANSAC-Regressor was used to find the slopes and this method of fitting does not provide uncertainties for the fitted parameters. It would be possible to calculate the uncertainty of the slope by using the least squares method for fitting after removing the outliers. But this was not done in this case, since we use the obtained effective viscosities to derive a representative effective viscosity using the median statistic (for its robustness against outliers) is used for the μ estimator. This is allowed if the underling distribution is symmetric and with finite mean has a median equal to its mean. This is the case if this estimator will vary like a normal distribution and thus the error will be calculated using the standard mean error.

Table 5.1: This table contains the effective viscosities η_{eff} of all the tracked particles from Figure 5.4 and Figure 5.5, which where calculated using Equation 12. Here is only the uncertainty due to actual temperature in the fluid considered in the measured effective viscosities. Using the median statistic and the standard mean error the estimator for the true $\hat{\eta}_{\text{eff}}$ is calculated.

	η_{eff}
Capture 1 Particle 1	$(0,63 \pm 0,30) \text{ mPa s}$
Capture 1 Particle 2	$(1,03 \pm 0,05) \text{ mPa s}$
Capture 1 Particle 3	$(0,97 \pm 0,05) \text{ mPa s}$
Capture 2 Particle 1	$(0,51 \pm 0,03) \text{ mPa s}$
Capture 2 Particle 2	$(0,87 \pm 0,04) \text{ mPa s}$
Capture 2 Particle 3	$(0,278 \pm 0,014) \text{ mPa s}$
$\hat{\theta}(\mu(\eta_{\text{eff}}))$	$0,87 \text{ mPa s}$
$\text{SEM}(\eta_{\text{eff}})$	$0,267 \text{ mPa s}$
$\Delta\eta_{\text{eff, Temperature}}$	$0,04 \text{ mPa s}$
$\hat{\eta}_{\text{eff}}$	$(0,9 \pm 0,4) \text{ mPa s}$

It is important to keep in mind that starts to dry, and this makes the particles drift towards an edge of the sample. This can be observed by a "dry-wall" that starts to move over the sample, as visible in Figure 5.6

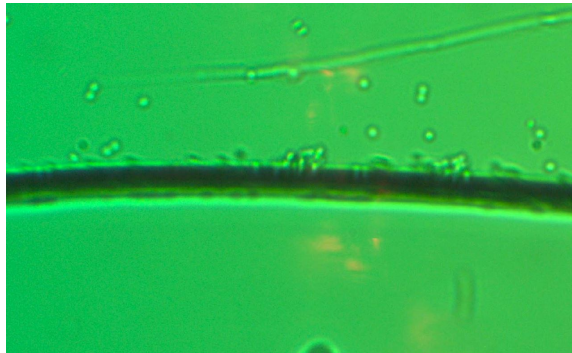


Figure 5.6: Dry-wall on the sample

5.2 Lasergun

For this part of the experiment the laser module without the telescope is added to the setup, the exact setup can be seen in Figure 3.1. From now on it is very important to keep in mind the principles of laser safety and use the laser safety googles, when the laser is turned on. When everything is prepared the laser can be switched on and the power can slowly be increased.

Once again the z-position of the stage needs to be increased until the focus of the laser becomes visible in the plane.

When the laser is in focus one can try to kick some particles with the laser beam by varying its power and moving it across the sample. This works on the principal of the radiation pressure, where the momentum of the photons is transferred to the particle. This was observed by the sudden movement of the particle once the laser beam hits it. These principles were discussed in detail in subsection 2.6. Another way of inducing particle motion will be discussed in subsection 5.7.

5.3 Trapping with laser

The aim of this experiment is to trap a particle inside the laser beam. This can be achieved by turning the laser to its highest power which is at the explicit case 100 mA and then bringing it close to a freely moving particle. The soaking of the particle can be observed. By moving the laser freely over the sample, the particle can be guided. By varying the power of the laser one can observe holding force increases with increased power. Furthermore, a size dependency was observed, smaller particles need less power to be trapped.

To also increase the power of the laser beam, the telescope cage, visible in Figure 3.1, is included to the setup, in order to focus the radiation pressure of the beam. There

are in total 3 positions where the laser beam is visible. It is important to work in the 3rd fokal plane. The interesting thing is, that the telescope didn't have a visible effect on the trapping strength. This was a bit odd and will be discussed in section 6.

Now one particle is trapped and slowly brought to a place on the sample, where also some other particles of approximately the same size are freely moving, as visible in Figure 5.7 and recorded to compare the movement of the trapped particle with the freely moving one.

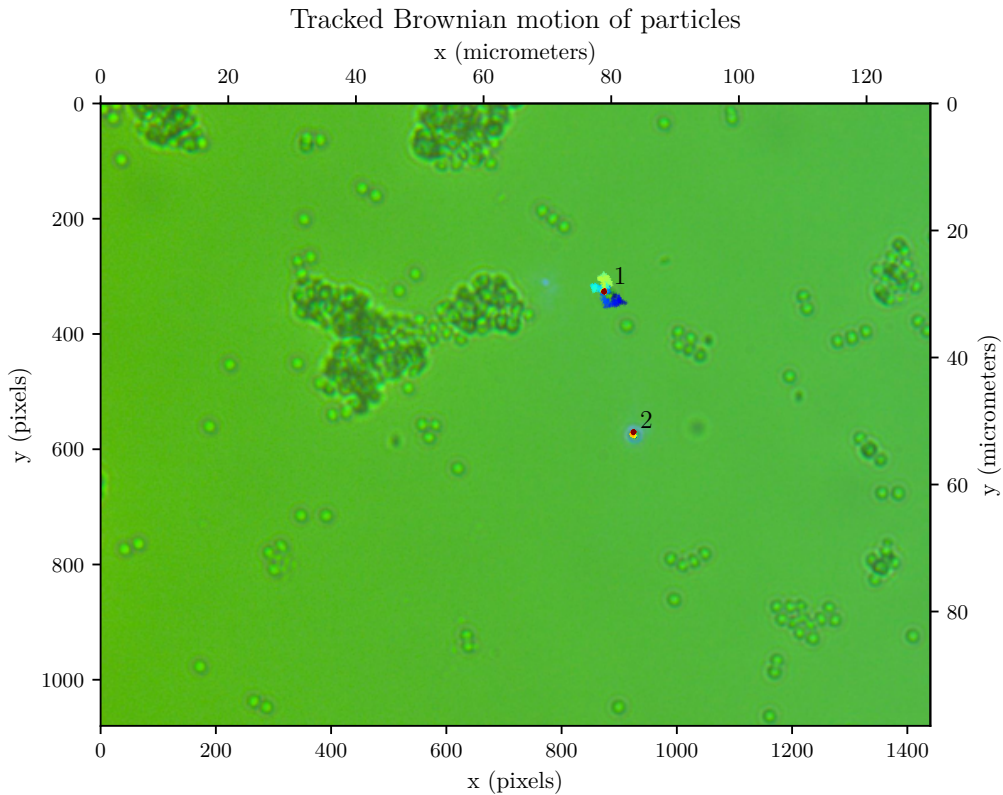


Figure 5.7: This figure contains the initial conditions of the tracked region displayed in the background and has the trajectories of the particles overlaid from cold to hot indicating the time evolution of the particles. Furthermore, the particles are labeled and plotted on an x, y coordinate grid. This tracking captured two particles first particle (1) is free and the second particle (2) is trapped.

If we use the captured trajectories and calculate the mean squared displacements for the trapped particle we can see the difference between trapped and free clearly in the following Figure 5.8.

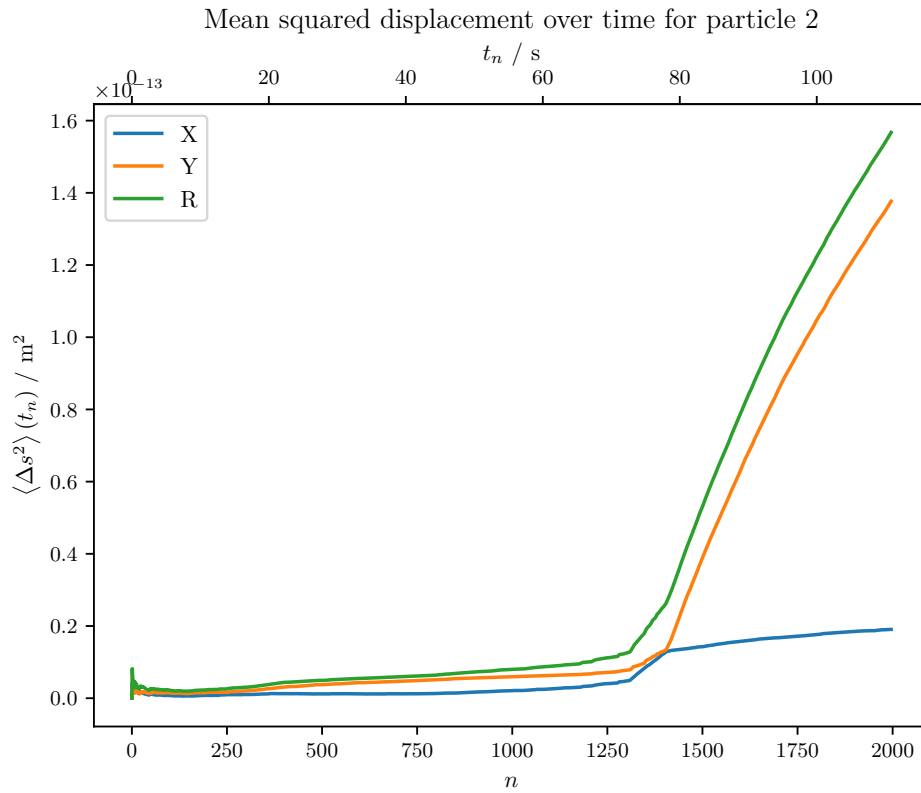


Figure 5.8: This figure one can see the time averaged mean squared displacements ($\langle \Delta s^2 \rangle (t_n)$) (averaged up to every time step t_n) in X and Y direction and the radial direction R for the trapped particle. The labels correspond to particles in Figure 5.7. Furthermore, the trapping was turned off at around step $n = 1250$ to contrast trapped vs free.

Next will be demonstrated that catching 2 particles at the same time is possible. When both particles are captured by the laser beam and the focus is regulated a bit, by adjusting the z-position of the sample, the particles can be stacked. In the image it looks like one particle, but when turning off the laser one can observe both particles drifting away, as visible in Figure 5.9.

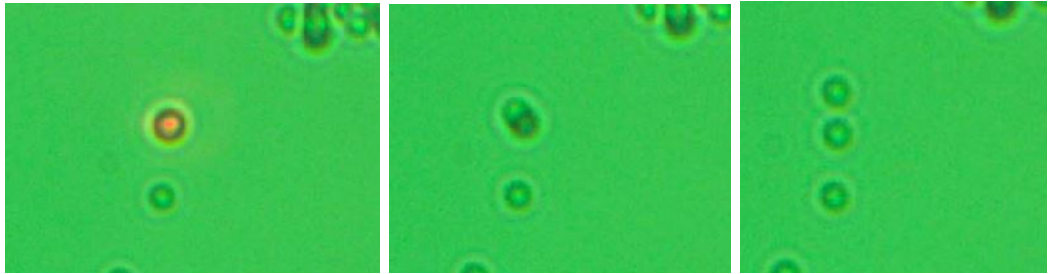


Figure 5.9: Snapshots of the video sequence of the trapping of 2 particles

5.4 Holding force

The aim of this experiment is to determine the holding force of the laser beam. Therefore, it is important that the focus of the laser is perfectly aligned. The aforementioned procedure was used to calibrate laser such that the force it has the maximal force. When multiple particles are bunched together and then the laser is able to align them this indicates, that this z-position is maximizing the holding force.

Next we find the limiting speed of the laser movement, where the particle are barely able to follow laser beam and remain trapped. To determine this the speed of the movement can be regulated in the menu of the controller. In order to find the correct speed we employed binary search, which means always try to divide the search space in every step. It is critical to remain at the same location while trying to find the correct speed, because at another location there might be some contamination on which the trapped particle could get stuck on. It is also important to keep in mind the drift due to the drying of the sample, as already mentioned in subsection 5.1. This procedure is now repeated for different laser powers and for 2 different particle sizes. The results are visible in Table 5.2.

Table 5.2: This table contains measured velocities and whether the particle remained trapped moving with the velocity at a certain laser power. All velocities are measured in mm s^{-1} . Here is max power of the laser diode 50 mW at 100 mA driver current. In the last row the chosen velocities for their respective categories are displayed. In the 50 % category the results were averaged and in the 100 % category the last binding velocity was used. The uncertainties are due the discretization of the actuator velocity, and the uncertainty are for all the velocities is $0,002 \text{ mm s}^{-1}$.

@50 % Power				@100 % Power			
$v_{\text{Big}}/\text{mm s}^{-1}$	Trapped?	v_{Small}	Trapped?	v_{Big}	Trapped?	v_{Small}	Trapped?
0,081	⊥	0,071	⊥	0,250	⊥	0,087	⊥
0,051	⊥	0,035	⊥	0,106	⊥	0,071	⊥
0,044	⊥	0,021	⊥	0,094	⊥	0,062	⊤
0,030	⊥	0,018	⊥	0,080	~		
0,025	⊥	0,016	⊥	0,076	~		
0,023	⊤	0,014	⊤	0,062	⊤		
0,021	⊤	0,011	⊤	0,053	⊤		
0,018	⊤	0,005	⊤	0,030	⊤		
$0,024 \pm 0,002$		$0,015 \pm 0,002$		$0,062 \pm 0,002$		$0,062 \pm 0,002$	

Using the measured velocities and the effective viscosities from the Table 5.1 one can calculate the holding forces by equating the frictional force with the holding force. The frictional force is described by law of Stokes, which is given by the equation:

$$|F_{\text{trap}}| = |k\Delta x| = F_{\text{Stoke}} = 6\pi R\eta_{\text{eff}}v \quad (13)$$

Table 5.3: This table contains the calculated holding forces F_{trap} using Equation 13 and the obtained value for the effective viscosity η_{eff} from Table 5.1 and the values for the critical holding velocities from Table 5.2.

	F_{trap}
Big @50 %	$(0,43 \pm 0,16) \text{ pN}$
Big @100 %	$(1,1 \pm 0,4) \text{ pN}$
Small @50 %	$(0,19 \pm 0,08) \text{ pN}$
Small @100 %	$(0,8 \pm 0,3) \text{ pN}$

5.5 Characterization of unknown sample

For this part the sample is changed. When removing the object holder it is important to go down in z-direction with the sample stage in order to do not hit the objective by changing the sample.

Now the objective colder can be cleaned and the new sample, labeled "unknown" placed on it.

When everything is attached and the laser beam is in focus again, one can try to search new particles. What one immediately sees is, that the new sample seems to contain particles that can absorb the laser beam, because one can "blow" them up.

What one can also observe with the bare eye is that the whole sample seems red, although there are also e few particles inside it, so the have a huge coloring effect.

Due to the huge impact of the laser light, one can state that the unknown sample contains metal particles. Since the particle are really small they are probably smaller then the wavelength of the light. This would also explain the purple colour of the sample due to Rayleigh regime.

5.6 Trapping of living organisms

For this part of the experiment one needs a sample with living bacteria on it. Therefore, a gulp of "ayran" gets diluted with water to make it transparent.

When everything is aligned and the laser is switched on again, one can try to find a bacterium. These bacteria can be easily detected due to their non-erratic movement. The bacteria have a major and minor axis and have cylindrical symmetry, once they enter the trap one can immediately observe, that it stops its movement and its major axis aligns with the laser beam, as visible in Figure 5.10. This happens, because this alignment is energetically favorable.

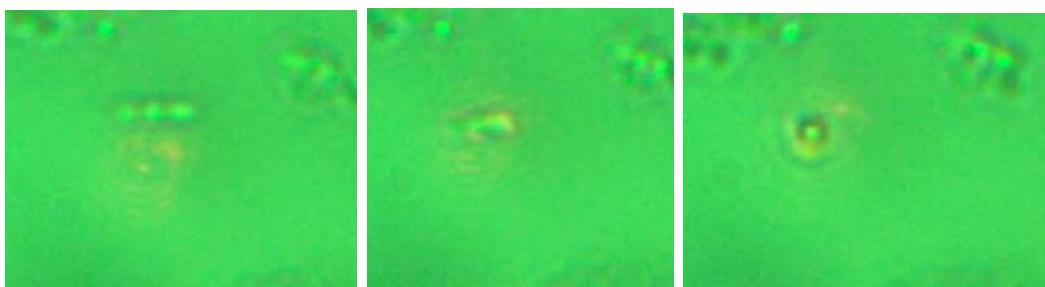


Figure 5.10: Snapshots of the video sequence of the alignment of a bacterium

These particles are probably staphylococci, because their more spherical nature than streptococci. They also build smaller chains and this is in agreement with the observation, that the longest chain was 3 long. Longer chains are improbable since they would build cluster, which are also sometimes visible in the sample.[2] In order to verify this, one could use a gram staining to differentiate between the two types of bacteria. Since they are gram positive, they would appear purple in the staining. This happens, because the cell wall is made of 40+ layers of murein, which is a peptidoglycan, and the staining particle sticks to it in the deep layers. After a cleaning cycle the dye would remain in the cell and the bacteria would appear purple. For bacteria with fewer layers, like gram negative bacteria, the dye would be washed out.[11]

5.7 Transfer of angular momentum

For this part of the experiment it is important to choose a particle, which has the necessary properties to transfer the angular momentum of the laser to it. This is the reason why, "vaterite" is used as a sample, since it birefringent (see subsubsection 2.6.1 for the other necessary properties for this behavior). To avoid pollution of the "ayran" sample this sample is placed on a new object holder.

When everything is aligned one navigates through the sample and searches for a particle that looks round but has a slight asymmetry, to later observe rotations of it.

To transfer the angular momentum of the laser to the particle one firstly needs to change the polarization from linear to circular light. This is done by holding a waveplate into the telescope and rotating it while observing the trapped particle.

Unfortunately the rotational effect was not as strong as expected. This can be explained, because many parameters need to fit in order to create that effect. Reasons for this will be discussed later in section 6.

6 Discussion

6.1 Microscope

As we can see the particles have been exhibiting Brownian motion. However, there seemed to be a preferred drift direction in Capture 2. These effects should result in a lower effective viscosity and this can also be seen when comparing the results from the Table 5.1 and the Figure 5.2 and Figure 5.3. This drift could be explained by the drying of the sample or the heating of the liquid due to the lamps radiation

or due to the forces present of the settling of cover glass. One could analyse this and quantify this qualitative observation by plotting a histogram of the movement directions and see the asymmetry.

6.2 Lasergun

In our setup it was sometimes possible by turning off and on the laser to only sometimes kick particles around. The laser focused enough such that trapping the particles was also possible, but this made it harder to impart momentum onto the particles.

6.3 Trapping with laser

Here it was possible to trap particles and even stack them. The desired effect of trapping particle and observing its reduced mobility was seen. The difference between the trapped and free particles was clearly visible in the Figure 5.8.

6.4 Holding force

The holding forces were calculated and the results are visible in Table 5.3. If one compares the holding with typical forces 10 pN to 20 pN per 100 mW power of the optical tweezers, one can see that the holding forces are an order of magnitude smaller. One can exclude thermal effect since the values of the effective viscosities (see Table 5.1) lie in the range of the literature values of 0,4 mPas to 1,5 mPas[<empty citation>]ViscosityWaterViscosity. The reason for the discrepancy is probably due to the fact that the optical tweezers were not properly focussed on the third focus plane. This would result in the particles being pulled to the glass interface. This would explain the reduced holding force due to scraping and that the effective viscosity is in agreement with the literature value. If this were the case this would mean that the drag velocities should be lower than expected, since no literature values were found for this setup, we cannot conclude this with complete certainty.

6.5 Characterization of unknown sample

Due to all the observations (color, electromagnetic interaction, size) it was concluded that the sample contains nanoparticles of gold, which was also confirmed by the tutor. The active region for gold particles of a size of 50 nm was simulated and

is visible in Figure 6.1. It is visible that there happens to be a big peak in the violett/blue region and also another one in the red area, which would in total result in the observed colour. What is also visible in the graph is that mainly the dipole part of the particle is present (orange in graph), which is a strong indicator for the Rayleigh regime.

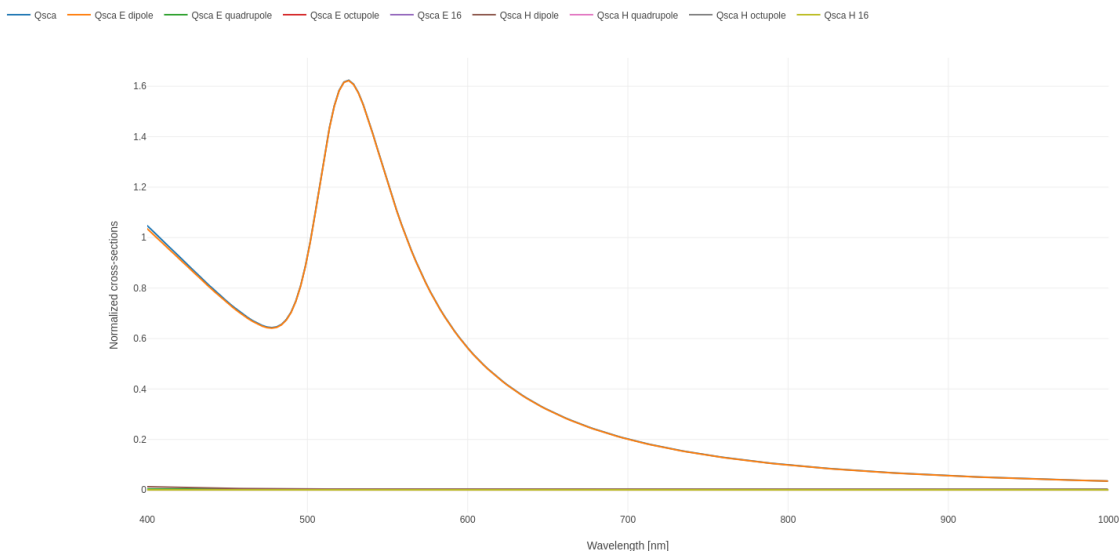


Figure 6.1: Simulated active region for gold particles of a size of 50 nm orange dipole contribution of scattering [9].

6.6 Trapping of living organisms

The desired effect of the trapping of the bacteria was observed. The bacteria aligned with the laser beam and stopped its movement. An attempt of the identification of the bacteria was made, but the results were not conclusive.

6.7 Transfer of angular momentum

Another effect that was not as strong as expected was the transfer of angular. This is also an indicator that the beam was not properly focused. This would also explain why the angular momentum transfer didn't work strongly. The scraping would reduce the mobility of the particles and would destroy the effect, as it did.

7 Conclusion

The setup for the microscope worked, which allowed us to track the motion of particles, as visible in Figure 5.2. Due to the connection between Brownian motion and Stokes' Law it was possible to determine the total viscosity $\hat{\eta}_{\text{eff}}$, which resulted in the following value.

$$\hat{\eta}_{\text{eff}} = (0,9 \pm 0,4) \text{ mPa s}$$

With the laser on this setup it was possible to kick and also trap the particles, and halt/reduce the Brownian motion, as visible in Figure 5.8.

It was also possible to calculate the holding force for different laser intensities and particle sizes, visible in Table 7.1

Table 7.1: This table contains the calculated holding forces F_{trap} from Table 5.3.

	F_{trap}
Big @50 %	(0,43 ± 0,16) pN
Big @100 %	(1,1 ± 0,4) pN
Small @50 %	(0,19 ± 0,08) pN
Small @100 %	(0,8 ± 0,3) pN

The unknown sample was characterized as gold particles, due to its color and electromagnetic interactions.

It was possible to trap and move a living organism, as visible in Figure 5.10, but it was not possible to conclusively classify it.

Unfortunately it was not fully possible to transfer angular momentum to a particle. Reasons for that are discussed in section 6.

Literaturverzeichnis

- [1] O. V. Angelsky et al. “Circular Motion of Particles Suspended in a Gaussian Beam with Circular Polarization Validates the Spin Part of the Internal Energy Flow”. In: *Optics Express* 20.10 (May 7, 2012), p. 11351. ISSN: 1094-4087. DOI: 10.1364/OE.20.011351. URL: <https://opg.optica.org/abstract.cfm?URI=oe-20-10-11351> (visited on 05/31/2024).
- [2] *Bakterienformen*. URL: <https://www.spektrum.de/lexikon/biologie-kom-pakt/bakterienformen/1192> (visited on 05/31/2024).
- [3] Peter Banzer. “LIGHT TWEEZERS - FROM OPTICAL LEVITATION AND TRACTOR BEAMS TO LIGHT-DRIVEN MICROMACHINES”. In: () .
- [4] Carlos J. Bustamante et al. “Optical Tweezers in Single-Molecule Biophysics”. In: *Nature Reviews Methods Primers* 1.1 (Mar. 25, 2021), p. 25. ISSN: 2662-8449. DOI: 10.1038/s43586-021-00021-6. URL: <https://www.nature.com/articles/s43586-021-00021-6> (visited on 05/31/2024).
- [5] A. Einstein. “Über Die von Der Molekularkinetischen Theorie Der Wärme Geforderte Bewegung von in Ruhenden Flüssigkeiten Suspendierten Teilchen”. In: *Annalen der Physik* 322.8 (Jan. 1905), pp. 549–560. ISSN: 0003-3804, 1521-3889. DOI: 10.1002/andp.19053220806. URL: <https://onlinelibrary.wiley.com/doi/10.1002/andp.19053220806> (visited on 05/31/2024).
- [6] A. Einstein. “Zur Quantentheorie Der Strahlung”. In: *Physikalische Zeitschrift* 18 (1917), pp. 121–128.
- [7] Adolf Fick. “Ueber Diffusion”. In: *Annalen der Physik* 170.1 (Jan. 1855), pp. 59–86. ISSN: 0003-3804, 1521-3889. DOI: 10.1002/andp.18551700105. URL: <https://onlinelibrary.wiley.com/doi/10.1002/andp.18551700105> (visited on 05/31/2024).
- [8] M. E. J. Friese et al. “Optical Alignment and Spinning of Laser-Trapped Microscopic Particles”. In: *Nature* 394.6691 (July 23, 1998), pp. 348–350. ISSN: 0028-0836, 1476-4687. DOI: 10.1038/28566. URL: <https://www.nature.com/articles/28566> (visited on 05/31/2024).
- [9] Konstantin Ladutenko et al. *Ovidiopr/Scattnlay: Small Bugfix for the Second Stable Release*. Version v2.0.1. Zenodo, Jan. 17, 2017. DOI: 10.5281/ZENODO.248729. URL: <https://zenodo.org/record/248729> (visited on 06/11/2024).
- [10] Anni Lehmuskerö et al. “Ultrafast Spinning of Gold Nanoparticles in Water Using Circularly Polarized Light”. In: *Nano Letters* 13.7 (July 10, 2013), pp. 3129–3134. ISSN: 1530-6984, 1530-6992. DOI: 10.1021/nl4010817. URL: <https://pubs.acs.org/doi/10.1021/nl4010817> (visited on 05/31/2024).
- [11] *Microbiological and hygenic discussion of the captured videos*. May 31, 2024.

- [12] M. Rothmayer et al. “Irregular Spin Angular Momentum Transfer from Light to Small Birefringent Particles”. In: *Physical Review A* 80.4 (Oct. 1, 2009), p. 043801. ISSN: 1050-2947, 1094-1622. DOI: 10.1103/PhysRevA.80.043801. URL: <https://link.aps.org/doi/10.1103/PhysRevA.80.043801> (visited on 05/31/2024).

List of Figures

2.1	Working principle of optical tweezers in mie regime	7
3.1	Total experimental setup	10
3.2	Optical setup	11
5.1	Object holder with placeholder	13
5.2	Capture 1 of particles	14
5.3	Capture 2 of particles	15
5.4	Time averaged mean squared displacements from the particles of the first capture	16
5.5	Time averaged mean squared displacements from the particles of the second capture	17
5.6	Dry-wall	19
5.7	Capture of trapped particle	20
5.8	Time averaged mean squared displacements of trapped particle . . .	21
5.9	Snapshots of the video sequence of the trapping of 2 particles . . .	22
5.10	Snapshots of the video sequence of the alignment of a bacterium . .	24
6.1	Simulated active region for gold particles	27

List of Tables

4.1	Used parts for the experiment	12
5.1	Collected effective viscosities	18
5.2	Measured velocities	23
5.3	Calculated holding forces	23
7.1	Calculated holding forces	28